This article was downloaded by:
On: *15 January 2011*
Access details: *Access Details: Free Access*
Publisher *Taylor & Francis*
Informa Ltd Registered in England and Wales Registered Number: 1072954 Registered office: Mortimer House, 37-41 Mortimer Street, London W1T 3JH, UK

Journal of Experimental Nanoscience
Publication details, including instructions for authors and subscription information:
http://www.informaworld.com/smpp/title~content=t716100757

Photo-deprotection patterning of self-assembled monolayers

Kevin Critchley[a]; Robert Ducker[b]; Jonathan P. Bramble[a]; Lixin Zhang[c]; Richard J. Bushby[c]; Graham J. Leggett[b]; Stephen D. Evans[a]
[a] School of Physics and Astronomy, University of Leeds, Leeds LS2 9JT, UK [b] Department of Chemistry, University of Sheffield, Sheffield S3 7HF, UK [c] Self Organising Molecular Systems (SOMS) Centre, University of Leeds, Leeds LS2 9JT, UK

To cite this Article Critchley, Kevin , Ducker, Robert , Bramble, Jonathan P. , Zhang, Lixin , Bushby, Richard J. , Leggett, Graham J. and Evans, Stephen D.(2007) 'Photo-deprotection patterning of self-assembled monolayers', Journal of Experimental Nanoscience, 2: 4, 279 — 290

To link to this Article: DOI: 10.1080/17458080701675780

URL: http://dx.doi.org/10.1080/17458080701675780

PLEASE SCROLL DOWN FOR ARTICLE

Full terms and conditions of use: http://www.informaworld.com/terms-and-conditions-of-access.pdf

This article may be used for research, teaching and private study purposes. Any substantial or systematic reproduction, re-distribution, re-selling, loan or sub-licensing, systematic supply or distribution in any form to anyone is expressly forbidden.

The publisher does not give any warranty express or implied or make any representation that the contents will be complete or accurate or up to date. The accuracy of any instructions, formulae and drug doses should be independently verified with primary sources. The publisher shall not be liable for any loss, actions, claims, proceedings, demand or costs or damages whatsoever or howsoever caused arising directly or indirectly in connection with or arising out of the use of this material.

Journal of Experimental Nanoscience,
Vol. 2, No. 4, December 2007, 279–290

Taylor & Francis
Taylor & Francis Group

Photo-deprotection patterning of self-assembled monolayers

KEVIN CRITCHLEY†, ROBERT DUCKER‡, JONATHAN P. BRAMBLE†, LIXIN ZHANG§, RICHARD J. BUSHBY§, GRAHAM J. LEGGETT‡ and STEPHEN D. EVANS*†

†School of Physics and Astronomy, University of Leeds, Leeds LS2 9JT, UK
‡Department of Chemistry, University of Sheffield, Brook Hill, Sheffield S3 7HF, UK
§Self Organising Molecular Systems (SOMS) Centre, University of Leeds, Leeds LS2 9JT, UK

(*Received August 2007; in final form September 2007*)

Downloaded At: 11:18 15 January 2011

Photo-deprotectable self-assembled monolayers (SAMs) provide a versatile platform for creating functional patterned surfaces. In this study, we present nanoscale photo-patterning, multi-component patterning, and a method for producing molecular gradients using photo-deprotectable SAMs. Nanoscale patterning of photo-deprotectable SAMs was achieved by coupling a UV laser (365 nm) through a scanning near field probe to produce nanoscale lines of ~40 nm, i.e. $\lambda/9$. Multi-component patterning was achieved by a two-stage method combining both microcontact printing and soft-UV photo-patterning. The example demonstrated in this study produced a three-component patterned surface with regions of CF_3, CH_3 and COOH/CF_3 functionality. The versatility of these photocleavable SAMs is further demonstrated by creating linear molecular gradients of two functionalities along a distance of ~25 mm. The use of 'soft' UV gives several advantages including the ability to pattern SAMs with micron-scale features over large areas quickly, with greater control over the photochemical reactions, and compatibility with existing lithographic facilities thus offering an effective alternative to other patterning methods such microcontact-printing or deep UV patterning.

Keywords: Multi-component patterns; SNOM lithography; Soft UV photo-patterning; self-assembled monolayers; Molecular gradients.

1. Introduction

Self-assembled monolayers (SAMs) formed from alkanethiol derivatives have proven to be excellent model systems for a wide range of fundamental studies [1–6]. The ability to produce "chemical" patterns on surfaces allows control over higher level assembly; for example, this makes it possible to selectively deposit conducting polymers [7, 8], control the orientation and nucleation of crystals [9], attach nanoparticles to designated regions

*Corresponding author. Email: s.d.evans@leeds.ac.uk

Journal of Experimental Nanoscience
ISSN 1745–8080 print/ISSN 1745–8099 online © 2007 Taylor & Francis
http://www.tandf.co.uk/journals
DOI: 10.1080/17458080701675780

of a surface [10–12], assemble biological molecules and cells [13, 14], align nematic liquid crystals [15, 16], and more. There are many methodologies for patterning SAMs including microcontact printing [17–21], dip-pen lithography [22, 23], ion-beam lithography [24], e-beam lithography [25–28], and scanning tunneling lithography [29, 30]. With the exception of microcontact printing, these techniques tend to be either time consuming and only suitable for small areas or require expensive instrumentation. However, another technique that can produce patterns over a large scale is ultraviolet (UV) photopatterning [31–35]. Deep UV photopatterning ($\lambda \leq 255\,nm$; $h\nu > 4.8\,eV$) of alkanethiol and organosilane SAMs was developed in the early 1990s and was used to create well-defined micron-scale features that could be used as templates for various reactions and assemblies [31–38]. The photopatterning mechanism of alkanethiol SAMs relies upon localised oxidation of thiolate bonds to form sulphonates (RS-Au + 3/2O2 $\rightarrow$ RSO3- + Au+) [34, 38–40]. The weakly bound sulphonates can then be easily rinsed away and the sample can be placed in a new alkanethiol solution to back-fill the irradiated areas. Similarly, deep UV light can be used to pattern organosilane SAMs [31–33, 36, 37]. This mechanism mainly involves the photocleavage of the C-Si bond. However, it is generally accepted that other photochemical reactions can occur when using deep UV. Chen *et al.* [41] investigated deep UV ($\lambda = 193\,nm$; $h\nu \sim 6.4\,eV$) photolysis with several aromatic silane derivatives and found that low doses C-N bonds were the primary cleavage pathway (68%) with the Si-C bond being secondary (32%). Although this can be used to an advantage, it is clear that more than one photochemical pathway occurs and, in some cases, this could leave the surface with 'non-specific' multiple functional groups.

Several researchers have demonstrated that photopatterning can be achieved using soft UV ($\lambda = 365\,nm$, $h\nu \sim 3.4\,eV$) light by incorporating photo-reactive ortho-nitrobenzyl chromophores [42–55]. At this wavelength, the photon energy is not sufficient to cause any significant photo-oxidisation of the SAM headgroups, and so we rely upon photochemistry to cleave the molecules at a designated bond to reveal new functionality. The advantage of this type of system is that no backfilling of the irradiated regions is required, i.e. reducing the number of steps to producing a pattern. The second advantage of this system is that 'soft' UV is a more mild form of radiation with which no ozone or oxygen free radicals are produced, rendering it compatible with biological molecules and making it possible to execute multiple exposures. We have previously reported two families of nitrobenzyl derivatives that form SAMs that can be photo-deprotected [42, 43]. The first system was an amine functionalised SAM that was 'protected' by a nitrobenzyl derivative with a semi-fluorinated tail group to produce CF_3 functionality. These SAMs were photo-deprotected to reveal amine functionality [44]. The second system reported was based on disulphide derivatives that contained nitrobenzyl groups. These were used to form complete SAMs that could be photo-deprotected to reveal carboxylic acid groups [56]. Reference 56 provides a detailed characterisation of the latter system using X-ray photoelectron spectroscopy, grazing angle Fourier transform infrared spectroscopy, wetting, and secondary ion mass spectroscopy. In this study, we present photopatterning techniques using the same disulphide photocleavable derivatives, **1** and **2**, as used in [56] figure 1. Compounds **1** and **2** both form SAMs that produce low surfaces energies (with advancing water contact angles of 117° and 112°, respectively). These hydrophobic SAMs

Downloaded At: 11:18 15 January 2011

Downloaded At: 11:18 15 January 2011

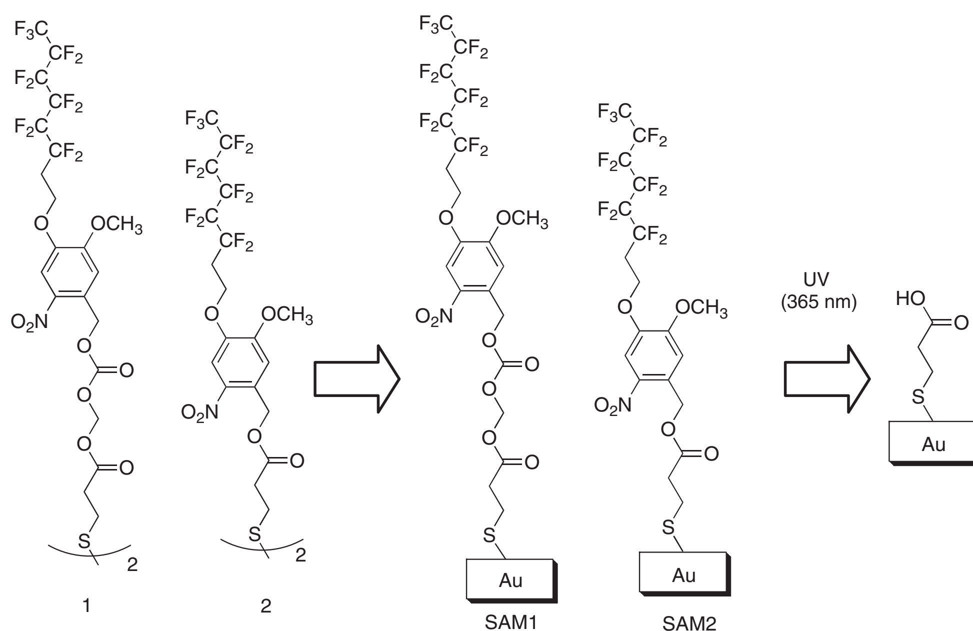

Figure 1. Compounds **1** and **2** can be both used to form SAMs on gold. Both **1** and **2** contain photo-cleavable units, which make it possible to remove the hydrophobic tail group using soft UV irradiation. Both SAM1 and SAM2 have similar surface properties after exposure. See [56] for further details of SAM1 and SAM2.

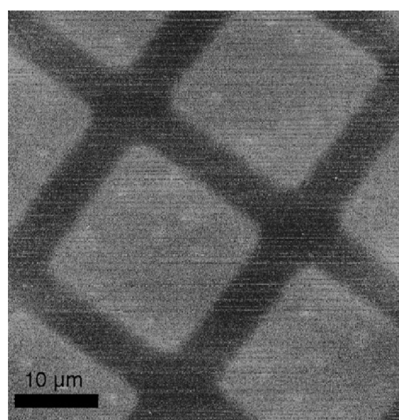

Figure 2. A lateral force microscopy image ($50 \times 50\,\mu m$) of SAM2 that has been exposed to UV light through a photomask to produce 20×20 micron squares. The dark regions represent 'low' friction from the CF_3 groups and the light regions represent 'high' friction associated with carboxylic acid functionality.

(SAM1 and SAM2) can be photo-deprotected using soft UV irradiation to reveal carboxylic acid groups figure 1 [56].

Photopatterns can be formed by irradiating the sample through a photomask. Figure 2 shows a lateral atomic force microscope (AFM) image of SAM2, which has

been exposed to 365 nm UV irradiation through a TEM grid. The higher friction regions are lighter which is indicative of presence of an increase in high-surface energy groups. The darker, lower friction regions, represent the unexposed SAM2 surface (CF_3 functionality). Patterns such as these can be produced routinely, but the pattern resolution is limited to the micron scale. In this study, we show for the first time that the SNOM can be coupled with a 'soft' UV ($\lambda = 365$ nm) source to produce high-resolution patterns on photo-deprotectable SAMs (SAM2). Furthermore, we also present a method for producing micron-scale multi-component patterns by combining both micro-contact printing and photo-deprotecting methodologies. Finally, we show that this system can also be used to produce linear molecular gradients.

2. Experimental

2.1 *Materials*

Dodecanethiol >98% (DDT), Dichloromethane 99.9% (DCM), hydrogen peroxide (27.5 wt.%), were used as received from Sigma-Aldrich. Sulfuric acid (98%) was supplied by Fisher Scientific. Glass microscope slides (thickness of 0.8 mm) were purchased from Agar and were cut approximately three quarters of the original length. Millipore Milli-Q water with a resistivity better than 18.1 MΩ cm was used throughout. High purity (99.99%) temper annealed gold wire (0.5 mm diameter) was supplied by Advent. Details of the synthesis of the compounds **1** and **2** used to form SAM1 and SAM2 can be found elsewhere [56].

Downloaded At: 11:18 15 January 2011

2.2 *Substrate preparation*

The glass microscope slides were first cleaned by ultrasonication for 15 minutes in a 10% solution of Decon90 in Milli-Q water. Each slide was rinsed with Milli-Q water for several minutes and then dried under a stream of nitrogen. The samples were ultrasonicated in dichloromethane for 15 minutes, removed and dried, rinsed under Milli-Q water, and immersed in piranha solution (70 : 30, v/v, $H_2SO_4 : H_2O_2$) for 10 minutes. *Caution: Piranha solution reacts violently with organic materials and should be treated with great care*. The substrates were then rinsed in Milli-Q grade water, dried under nitrogen, and placed in an Edwards Auto 306 thermal evaporator. A 200 nm gold layer was thermally deposited ($0.1\ nm.s^{-1}$) onto a chromium adhesion layer (5 nm), at a base pressure of approximately 1×10^{-6} mbar. The gold-coated samples were cleaned immediately prior to use by placing them in freshly prepared piranha solution for 1–2 minutes, followed by a rinse with Milli-Q water. SAM Adsorption: SAM1 and SAM2 were formed by immersing the gold-coated slides in 0.5 mM solution (DCM) for 16 h, at 23 °C. The SAMs were removed from solution, rinsed with DCM, dried with a nitrogen stream, rinsed with Milli-Q grade water and again dried.

2.3 *UV irradiation of SAMs*

Unless stated otherwise, a 365 nm UV lamp (Blak-Ray Model B 100 AP) with a nominal power (at the sample) of $7\ mWcm^{-2}$ was used to irradiate the samples, in air,

for 3600 s. After the UV irradiation, samples were rinsed with DCM, followed by Milli-Q water, and finally dried under a stream of nitrogen.

2.4 *Scanning near-field photolithography*

The nanoscale photolithography was achieved by coupling a tuneable laser (365 nm) to a Thermomicroscopes Aurora III near field scanning optical microscope fitted with a fused silica fibre probe (Veeco).

2.5 *X-ray photoelectron spectroscopy*

Spectra were obtained using a Thermo Electron Corporation ESCA Lab 250 with a chamber pressure maintained below 1×10^{-9} mbar during acquisition. A monochromated Al Kα X-ray source (15 kV; 150 W) irradiated the samples, with a spot diameter of approximately 0.5 mm. The spectrometer was operated in Large Area XL magnetic lens mode using a pass energy of 20 eV for detailed scans of the F 1s and Au 4f regions, respectively. The spectra were obtained with an electron take-off angle of 90°. High-resolution spectra were fitted using Avantage (Thermo VG software package) peak fitting algorithms. All spectra have been normalized to the Au $4f_{7/2}$ peak.

Downloaded At: 11:18 15 January 2011

3. Results and discussion

3.1 *Nanoscale patterning*

In this paper, we demonstrate for the first time that the SNOM can be used to create nanolines using photo-deprotectable SAMs using soft UV (365 nm) irradiation. SAM2 (figure 1) was formed from solution onto a gold substrate. Nanoscale features were produced by rastering the UV ($\lambda = 365$ nm) laser coupled SNOM tip across the surface figure 3(a). Figure 3(b) shows a lateral force AFM image of a nanoline drawn onto the SAM surface. A nominal intensity of 1.5 mW was coupled into the SNOM optical fiber and a tip raster speed of 0.1 μms^{-1} was employed to generate a nanoline with a full-half maximum width (FHMW) of $\sim$40 nm, representing a resolution of $\lambda/9$, significantly beyond the conventional Rayleigh limit. The lighter regions (lines) indicate higher friction, which is consistent with the presence of carboxylic acid groups at the surface. The grains within the image are from the roughness of the thermally evaporated gold. Interestingly, the line width appears to be similar to the grain size. Figure 3(c) shows slightly larger features, with a FHMW of approximately 150 nm. These lines were generated by supplying a nominal laser intensity of 5 mW to the SNOM and a raster rate of 0.2 μms^{-1}. The width of the nanolines is a complicated relationship between the geometry of the SNOM tip, the intensity, alignment of the UV laser, the raster speed, and the tip sample separation. The conditions need to be optimised each time the tip is replaced. The 40 nm line presented is the smallest FHMW measured for a UV deprotection SAM to date and compares well to SNOM patterning using deep UV light [57–59].

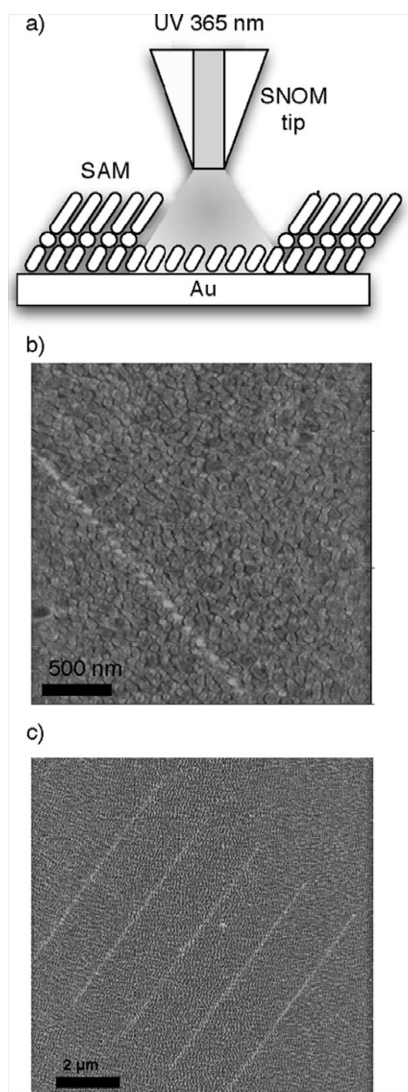

Figure 3. (a) A schematic of a scanning near-field optical microscope (SNOM) tip used to pattern below the conventional diffraction limit (Not to scale). (b) A lateral force image of a nanoline drawn into SAM2 using a soft-UV ($\lambda = 365$ nm) SNOM. The FHWM of this line was 40 nm. (c) A lateral force image of a series of nanolines drawn onto SAM2 with an average line width of 150 nm.

3.2 *Multi-component patterning*

SAMs that are designed to photo-deprotect under soft UV light can be combined with simple alkanethiol SAMs (e.g., Octodecanethiol [44]) to produce new geometries not easily achieved using deep UV light or microcontact printing alone. Ryan *et al.* [45] demonstrated that SAMs of methoxy-nitrobenzyl derivatives could be photopatterned to produce 'three-component' surface functionality. In their case, a mask was fabricated that contained three components; one that was transparent (transmitted

Downloaded At: 11:18 15 January 2011

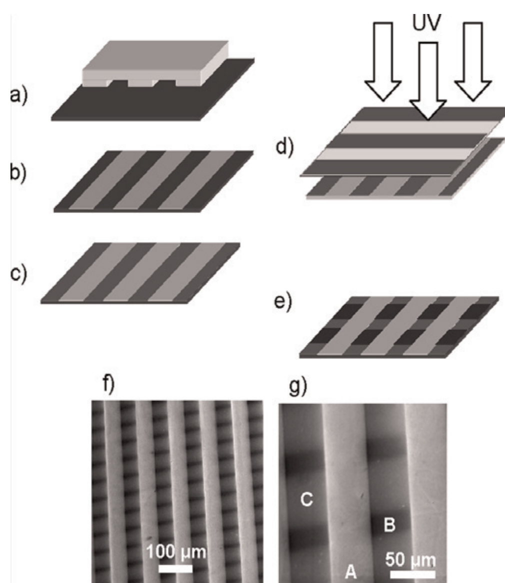

Figure 4. Fabricating a multi-component functional surface. The gold surface is first stamped (a) with octadecanethiol (ODT) (b). The stamped surface is backfilled with the CF_3 functionalised photo-deprotectable SAM (c). The two-component surface was then exposed to soft-UV through a striped mask perpendicular to the stamped stripes (d). The ODT component was not affected by soft UV light, while SAM1 is partially photo-deprotected (e). This leaves the surface with three components; A ODT, B -CF_3 functionalised 'protected' SAM, C and photo-deprotected SAM (-COOH -CF_3). (f) and (g) scanning electron microscopy images of the patterned SAMs.

Downloaded At: 11:18 15 January 2011

365 and 220 nm light); the second blocked 220 nm light; and the third blocked both 220 and 365 nm light. The mask was then placed in contact with the surface and exposed to 365 nm and 220 nm irradiation, simultaneously. The region under the opaque component of the mask remained unchanged. The region that was exposed to 220 nm light was photo-oxidised, allowing one to displace these molecules with another thiol derivative. The region exposed to only 365 nm was deprotected to reveal a different functionality. This meant it was possible to produce three-component chemically patterned surfaces [45]. Here, we demonstrate a new method of producing three-component surfaces based on a two-step process that is both versatile and simple. In the first step (figure 4(a–c)), octadecanethiol (ODT) was micro-contact printed onto the gold to create stripes of ODT using standard methodology [17]. The ODT striped substrate was placed into a solution containing the photo-deprotectable SAM1 material to back-fill the 'bare' gold regions. In the third step (figure 2(d–e)), a photomask was placed on the surface of the sample so that the masked lines were approximately perpendicular to that of the stamped pattern was then exposed to 365 nm light. The irradiated SAM1 molecules were partially photo-deprotected to reveal carboxylic acid groups ($COOH/CF_3$). This produced surfaces with three-components of functionality. It is widely known that the tail groups of self-assembled monolayers can modify the work function of substrates by up to $\sim$1 eV (demonstrated using Kelvin probe techniques) [60–62]. This effect is attributed to direction and magnitude of the normal

component of the net dipole moment of the molecules within the SAM. For example, the -CH_3 group of an alkanethiol molecule within an ODT SAM has a dipole moment directed from the air/SAM interface towards the SAM/substrate interface. This effect can be imaged when examining a patterned SAM using a scanning electron microscope (SEM). Figures 4(f,g) show SEM images of the three-component SAM produced. Regions A, B and C represent the CH_3, CF_3, and COOH functionality, respectively. The brightest regions corresponds to those with the lowest work (CH_3) function and this reflects that expected, since the work functions of the samples are in the relative order; $CH_3 < COOH < CF_3$.

3.3 *Molecular gradient*

The ability to pattern a surface with different functional groups increases the potential applications of SAMs. There are several ways to produce SAM gradients in the literature [63–74]. Soft X-rays [64] can be used by varying the exposure across the sample. Alternatively, gradients can be made by; producing a temperature gradient across that in turn affects the adsorption kinetics [65], by diffusion methods [66–71], by contact printing gradients [72], or by using deep UV/Ozone and a variable density filter on silane SAMs [73, 74]. In the latter case, a SAM is formed on a substrate and is exposed through a gradient density filter. The deep UV/Ozone cleaves and oxidises the SAM producing hydrophilic groups to form a hydrophobic to hydrophilic gradient surface [74]. In this study, we used the photo-deprotectable SAM1 (figure 1), and exposed the sample to soft UV (365 nm) through a quartz gradient density filter (Thorlabs). The variable density filter comprised of quartz glass with a metal film, which increased in thickness linearly with position. From Beer's law the expected transmission as a function of position, was expected to closely follow an exponential decay. This was confirmed by using a spectroscopic ellipsometer in transmission mode (figure 5(a)) where the data is presented on a log scale. With the exception of the first few millimeter the curve fits well to an exponential decay function. These data were used to produce a transmission function for the modelling. The photolysis kinetics of SAM1 were previously studied, and are known to also follow a exponential decay function [56]. By using the photo-deprotection kinetics model from [56] and using the transmission function of the variable density filter allows the system to be modeled as a function of time. The modelling showed that the sample would have approximately a linear gradient of functionality at approximately three hours. Exposing the sample for too long 'saturates' at the high transmission end and shortens the length of the gradient region. In this experiment SAM1 was exposed through the variable density filter for 10800 s. The surface was analysed along the length of the sample using X-ray photoelectron spectroscopy (XPS) by acquiring data automatically in 'line' mode. The F 1s/Au 4f integrated intensity ratio was normalised to unexposed regions to determine the fraction of 'protected' moieties as a function of position along the sample (figure 5(b)). At small separation (0–5 mm) only $\sim$45% of the SAM molecules remain protected. This flat region (0–5 mm) closely coincides with the 'flat' region of transmission through the variable density filter, where the sample has received largest dose of UV light. The next 25 mm, (5–30 mm) was found to be almost linear gradient and is fitted to a straight line (dashed) in figure 5(b). Above 30 mm, the datum points

Downloaded At: 11:18 15 January 2011

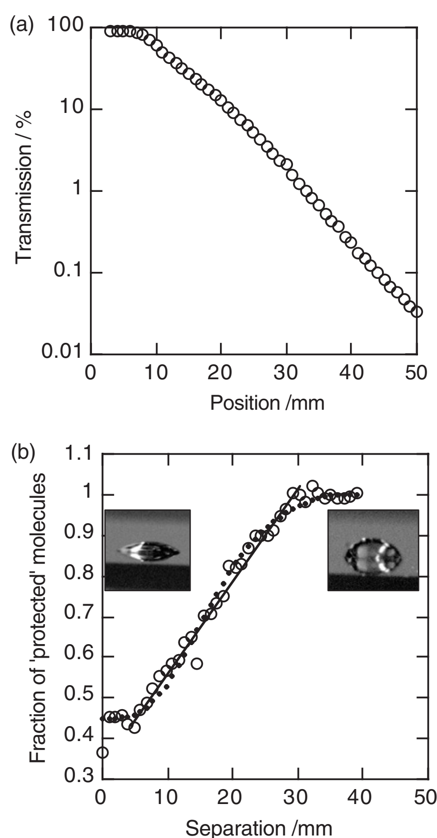

Figure 5. (a) The transmission function of the variable density filter at 365 nm. The y-axis is presented logarithmically to show that the transmission exponentially decay with position. (b) The molecular gradient of SAM1, after 3 h exposure through the variable density filter, as determined from the F 1s/Au 4f integrated area ratio (open circles). The filled dots represent the modeled data. The solid black line is a guide to the eye through the gradient region. The plot shows an increase in the number of protected groups as a function of position across the sample (left to right). The inserts are images of the hexadecane droplets placed on either end of the gradient.

Downloaded At: 11:18 15 January 2011

flatten off, this is where the sample has received least light and the SAM groups remain protected. The entire data range was fitted to a theoretical model. The fraction of groups that remain 'protected' at a time, t, and separation, x along the sample is given by (equation 1),

$$\phi(x,t) = e^{-(k_1+k_2)T(x+a)t} + \frac{k_2}{k_1+k_2}\left[1 - e^{-(k_1+k_2)T(x+a)t}\right], \quad (1)$$

where, k_1, is the photoreaction rate for photodeprotection, k_2 is the 'competing reaction' (reduction of nitro to amine preventing deprotection [56]), and $T(x)$ is the transmission as a function of position along the gradient density filter. The rate constants k_1 and k_2, from out previous work, were found to be $3.3 \times 10^{-4}\,s^{-1}$ and $2.9 \times 10^{-4}\,s^{-1}$, respectively. The variable, a, was included to allow for the fact that the

gradient does not start exactly at the edge of the sample. Assumptions made in the modelling were that the light source was stable and the intensity was evenly distributed across the surface. This method may prove to be a suitable method of assessing the kinetics of surface photoreactions for other systems since in theory only one sample is needed to follow a full series of doses of light. The inserts in figure 5(b) shows droplets of hexadecane place at each end of the gradient. The contact angles of the HD droplets increased from left to right. Interestingly, droplets could be moved down the molecular gradient, but not easily up the gradient (rather similar to a ratchet mechanism). The surface energy contrast was not sufficient to cause droplets to move spontaneously while the sample was held level. We are currently working on surfaces that will generate larger contrasts.

4. Conclusions

There are currently only a limited number of ways one can produce nanoscale patterned surfaces and study demonstrates the first example of nanoscale photo-deprotection patterning using 'soft UV'. The best example gave lines with a width of 40 nm. Larger line widths can be produced routinely on both SAM1 and SAM2. We are continuing to study this technique on this, and similar systems. We believe that nanoscale patterning of amine and carboxylic acid will be useful for self-assembling biological molecules. Multi-component patterning of surfaces allows one to make three or more potential attachment sites in an ordered manner across a larger area can be achieved easily using the two-stage method presented here. One can also have a two component 'protected pattern' ready for subsequent use later. This can achieved by first stamping your first thiol, back-filling with a photo-deprotectable SAM. When the pattern is required the entire sample can be exposed to UV light to 'deprotect' the pattern. Finally we show that molecular gradients can also be produced using photo-deprotectable SAMs. There is no doubt of the potential uses of these techniques and this system, however, the greatest problem we have is the relatively low photoreaction yield (~55%), which restricts the contrast achievable between the fully 'deprotected' and 'protected' regions. This is a matter that is under further investigation.

Downloaded At: 11:18 15 January 2011

Acknowledgements

We thank the Seiko-Epson Corporation for funding of this study. K.C. was also grateful to EPSRC for their financial support.

References

[1] A. Ulman. *An Introduction to Ultrathin Organic Films from Langmuir-Blodgett to Self-assembly*, Academic Press, Boston, London (1991).
[2] A. Ulman. *Chem. Rev*, **96**, 1533 (1996).
[3] A. Ulman. *Organic Thin Films and Surfaces - Directions for the Nineties*, Academic Press, New York (1995) Vol. 20.
[4] R.H. Tredgold. *Order in Organic Films*, Cambridge University Press, Cambridge (1994).

[5] J.C. Love, L.A. Estroff, J.K. Kriebel, R.G. Nuzzo, G.M. Whitesides. *Chem. Rev.*, **105**, 1103 (2005).
[6] J.J. Gooding, F. Mearns, W. R. Yang, J. Q. Liu. *Electroanalysis*, **15**, 81 (2003).
[7] Z.Y. Huang, P.C. Wang, A.G. MacDiarmid, Y.N. Xia, G. Whitesides. *Langmuir*, **13**, 6480 (1997).
[8] L.F. Rozsnyai, M.S. Wrighton. *Chem. Mat.*, **8**, 309 (1996).
[9] J. Aizenberg, A.J. Black, G.H. Whitesides. *J. Am. Chem. Soc.*, **121**, 4500 (1999).
[10] K. Tsuboi, K. Kajikawa. *Appl. Phys. Lett.*, **88**, 103102 (2006).
[11] P.M. Mendes, S. Jacke, K. Critchley, J. Plaza, Y. Chen, K. Nikitin, R.E. Palmer, J.A. Preece, S.D. Evans, D. Fitzmaurice. *Langmuir*, **20**, 3766 (2004).
[12] S. Sun, K.S.L. Chong, G.J. Leggett. *Nanotechnology*, **16**, 1798 (2005).
[13] S. Sun, M. Montague, K. Critchley, M.S. Chen, W.J. Dressick, S.D. Evans, G.J. Leggett. *Nano Lett.*, **6**, 29 (2006).
[14] K. Wadu-Mesthrige, S. Xu, N.A. Amro, G.Y. Liu. *Langmuir*, **15**, 8580 (1999).
[15] Y.L. Cheng, D.N. Batchelder, S.D. Evans, J.R. Henderson, J.E. Lydon, S.D. Ogier. *Liq. Crys.*, **27**, 1267 (2000).
[16] S.D. Evans, H. Allinson, N. Boden, T.M. Flynn, J.R. Henderson. *J. Phys. Chemistry B*, **101**, 2143 (1997).
[17] Y.N. Xia, G.M. Whitesides. *Annu. Rev. Mater. Sci*, **28**, 153 (1998).
[18] C.S. Chen, M. Mrksich, S. Huang, G.M. Whitesides, D.E. Ingber. *Biotechn. Prog.*, **14**, 356 (1998).
[19] R.J. Jackman, J.L. Wilbur, G.M. Whitesides. *Science*, **269**, 664, (1995).
[20] J.L. Wilbur, A. Kumar, E. Kim, G.M. Whitesides. *Advanc. Mat.*, **6**, 600 (1994).
[21] B. Michel, A. Bernard, A. Bietsch, E. Delamarche, M. Geissler, D. Juncker, H. Kind, J.P. Renault, H. Rothuizen, H. Schmid, P. Schmidt-Winkel, R. Stutz, H. Wolf. *IBM J. Res. Dev*, **45**, 697 (2001).
[22] R.D. Piner, J. Zhu, F. Xu, S.H. Hong, C.A. Mirkin. *Science*, **283**, 661 (1999).
[23] P.E. Sheehan, L.J. Whitman. *Phys. Rev. Lett*, **88**, 156104 (2002).
[24] E.T. Ada, L. Hanley, S. Etchin, J. Melngailis, W.J. Dressick, M.S. Chen, J.M. Calvert. *J. Vac. Sci. Technol. B*, **13**, 2189 (1995).
[25] A. Kuller, M.A. El-Desawy, V. Stadler, W. Geyer, W. Eck, A. Golzhauser. *J. Vac. Sci. Technol. B*, **22**, 1114 (2004).
[26] E. Balaur, T. Djenizian, R. Boukherroub, J.N. Chazalviel, F. Ozanam, P. Schmuki. *Electrochem. Commun.*, **6**, 153 (2004).
[27] T. Weimann, W. Geyer, P. Hinze, V. Stadler, W. Eck, A. Golzhauser. *Microelectron. Eng.*, **57**, 903 (2001).
[28] A. Golzhauser, W. Geyer, V. Stadler, W. Eck, M. Grunze, K. Edinger, T. Weimann, P. Hinze. *J. Vac. Sci. Technol. B*, **18**, (2000).
[29] C.B. Ross, L. Sun, R.M. Crooks. *Langmuir*, **9**, 632 (1993).
[30] R.K. Smith, P.A. Lewis, P.S. Weiss. *Prog. Surf. Sci.*, **75 1**, (2004).
[31] C.S. Dulcey, J.H. Georger, V. Krauthamer, D.A. Stenger, T.L. Fare, J.M. Calvert. *Science*, **252**, 551 (1991).
[32] J.M. Calvert, S.L. Brandow, M.S. Chen, W.J. Dressick, C.S. Dulcey, T.S. Koloski, D.A. Stenger. *Abstr. Pap. Am. Chem. Soc.*, **205**, 11 (1993).
[33] W.J. Dressick, J.M. Calvert. *Jpn. J. Appl. Phys*, **32**, 5829 (1993).
[34] J. Huang, J.C. Hemminger. *J. Am. Chem. Soc*, **115**, 3342 (1993).
[35] M.J. Tarlov, D.R.F. Burgess, G. Gillen. *J. Am. Chem. Soc*, **115**, 5305 (1993).
[36] J.M. Calvert, M.S. Chen, C.S. Dulcey, J.H. Georger, M.C. Peckerar, J.M. Schnur, P.E. Schoen. *J. Vac. Sci. Technol. B*, **9**, 3447 (1991).
[37] H. Sugimura, K. Ushiyama, A. Hozumi, O. Takai. *Langmuir*, **16**, 885 (2000).
[38] J.Y. Huang, D.A. Dahlgren, J.C. Hemminger. *Langmuir*, **10**, 626 (1994).
[39] N.J. Brewer, S. Janusz, K. Critchley, S.D. Evans, G.J. Leggett. *J. Phys. Chem. B*, **109**, 11247 (2005).
[40] N.J. Brewer, R.E. Rawsterne, S. Kothari, G.J. Leggett. *J. Am. Chem. Soc*, **123**, 4089 (2001).
[41] M.-S. Chen, C.S. Dulcey, L.A. Chrisey, W.J. Dressick. *Adv. Funct. Mater*, **16**, 774 (2006).
[42] H. Fukushima, H. Takiguchi, T. Shimoda, R.J. Bushby, S.D. Evans, J.P. Jeyadevan, K. Critchley, *GB, UK and EP Patent GB 2413553, US 2005245739, EP 1610176* (2004).
[43] H. Fukushima, H. Takiguchi, T. Shimoda, R.J. Bushby, S.D. Evans, J.P. Jeyadevan, K. Critchley, *UK Patent US 2005245739, GB 2413553* (2004).
[44] K. Critchley, J.P. Jeyadevan, H. Fukushima, M. Ishida, T. Shimoda, R.J. Bushby, S.D. Evans. *Langmuir*, **21**, 4554 (2005).
[45] D. Ryan, A.P. Parviz, V. Linder, V. Semetey, S.K. Sia, J. Su, M. Mrkich, G.M. Whitesides. *Langmuir*, **20**, 9080 (2004).
[46] V.N.R. Pillai. *Synthesis-Stuttgart*, **1**, 1 (1980).
[47] C.G. Bochet. *J. Chem.Soc. Perkin Trans.*, **1**, 125 (2002).
[48] A.d. Campo, D. Boos, H.W. Spiess, U. Jonas. *Angew. Chem. Int. Ed*, **44**, 4707 (2005).
[49] B. Zhao, J.S. Moore, D.J. Beebe. *Anal. Chem*, **74**, 4259 (2002).

Downloaded At: 11:18 15 January 2011

[50] B. Zhao, J.S. Moore, D.J. Beebo. *Langmuir*, **19**, 1873 (2003).
[51] U. Jonas, A. del Campo, C. Kruger, G. Glasser, D. Boos, Proceedings of the National Academy of Sciences of the United States of America, 99, 5034 (2002).
[52] G.H. McGall, A.D. Barone, M. Diggelmann, S.P.A. Fodor, E. Gentalen, N. Ngo. *J. Am. Chem. Soc*, **119**, 5081 (1997).
[53] M. Nakagawa, K. Ichimura. *Colloid Surf. A-Physicochem. Eng. Asp*, **204**, 1 (2002).
[54] J. Jennane, T. Boutros, R. Giasson. *Canadian Journal of Chemistry-Revue Canadienne De Chimie*, **74**, 2509 (1996).
[55] E. Besson, A.-M. Gue, J. Sudor, H. Korri-Youssoufi, N. Jaffrezic, J. Tardy. *Langmuir*, **22**, 8346 (2006).
[56] K. Critchley, L. Zhang, H. Fukushima, M. Ishida, T. Shimoda, R.J. Bushby, S.D. Evans. *J. Phys. Chem. B*, **110**, 17167 (2006).
[57] S. Sun, G.J. Leggett. *Nano Lett.*, **2**, 1223 (2002).
[58] S. Sun, K.S.L. Chong, G.J. Leggett. *J. Am. Chem. Soc.*, **124**, 2414 (2002).
[59] S. Sun, G.J. Leggett. *Nano Lett.*, **4**, 1381 (2004).
[60] S.D. Evans, A. Ulman. *Chem. Phys. Lett.*, **170**, 462 (1990).
[61] H. Sugimura, K. Hayashi, N. Saito, O. Takai, N. Nakagiri. *Jpn. J. Appl. Phys. Part 2 - Lett*, **40**, L174 (2001).
[62] J. Lu, L. Eng, R. Bennewitz, E. Meyer, H.J. Guntherodt, E. Delamarche, L. Scandella. *Surf. Interface Anal.*, **27**, 368 (1999).
[63] A.D. Price, D.K. Schwartz. *Langmuir*, **22**, 9753 (2006).
[64] R. Klauser, C.H. Chen, M.L. Huang, S.C. Wang, T.J. Chuang, M. Zharnikov. *J. Electr. Spectro. Rela. Pheno.*, **144**, 393 (2005).
[65] A. Shovsky, H. Schonherr. *Langmuir*, **21**, 4393 (2005).
[66] H. Elwing, S. Welin, A. Askendahl, U. Nilsson, I. Lundstrom. *J. Colliod Interface Sci*, **119**, 203 (1987).
[67] M.K. Chaudhury, G.M. Whitesides. *Science*, **256**, 1539 (1992).
[68] T.G. Ruardy, J.M. Schakenraad, H.C. van der Mei, H.J. Busscher. *Surf. Sci. Rep*, **29**, 1 (1997).
[69] B. Liedberg, P. Tengvall. *Langmuir*, **11**, 3821 (1995).
[70] M. Lestelius, I. Engquist, P. Tengvall, M.K. Chaudhury, B. Liedberg. *Colloid Surf. B-Biointerfaces*, **15**, 57 (1999).
[71] J. Genzer, K. Efimenko, D.A. Fischer. *Langmuir*, **22**, 8532 (2006).
[72] T. Kraus, R. Stutz, T.E. Balmer, H. Schmid, L. Malaquin, N.D. Spencer, H. Wolf. *Langmuir*, **21**, 7796 (2005).
[73] K. Loos, S.B. Kennedy, N. Eidelman, Y. Tai, M. Zharnikov, E.J. Amis, A. Ulman, R.A. Gross. *Langmuir*, **21**, 5237 (2005).
[74] S.V. Roberson, A.J. Fahey, A. Sehgal, A. Karim. *Appl. Surf. Sci.*, **200**, 150 (2002).

Downloaded At: 11:18 15 January 2011